A SENSITIVITY ANALYSIS ON GLARE DETECTION PARAMETERS

Mandana Sarey Khanie[1], Yiyuan Jia[2], Jan Wienold[1], Marilyne Andersen[1]
[1]Interdisciplinary Laboratory of Performance-Integrated Design (LIPID),
École Polytechnique Fédérale de Lausanne (EPFL), Switzerland
[2]College of Architecture, Georgia Institute of Technology, Atlanta, USA
Contact: mandana.sareykhanie@epfl.ch

ABSTRACT

Existing methods for glare-free daylighting rely on analyses of rendered images of physically based lighting simulations for predicting potential glare risks in a given lighting scenario. A major challenge in these analyses lies in the image-processing steps.
The objective of this study is to establish a sensitivity analysis on two influential parameters "threshold multiplier" and "search radius" that are set by the user in the evaluation process. High dynamic range (HDR) images captured during two sets of experiments were processed using 15 combinations for the two parameters in order to derive the glare impact. The glare impacts were then compared to the recorded subjective assessments. The results indicate the sensitivity of the two parameters.

INTRODUCTION

Maximising daylight access in order to enhance the indoor environment quality while maintaining a glare-free indoor environment is an ongoing challenge for daylighting design. Glare is a discomfort sensation that is produced as a result of greater variation of luminance across the visual field than the one that the eye is adapted to (Boyce, 2014). Due to no immediate physiological constrains and no visual impairment, this type of glare is still less understood and an on-going research is being performed (Boyce, 2014; Clear, 2012; Vos, 1999). What we know is that this type of discomfort sensation is one of the main drivers for building users' interaction with the façade settings (Dubois, 2003; Galasiu and Veitch, 2006), which consequently can change the building's performance over time. Optimised integration of glare-free daylight solutions thus proves to be crucial for a sustainable building design.

The most recent methods for glare-free daylighting design rely on analyses of high dynamic (HDR) range images. HDR images are produced by multiple-exposure image capture (taken from the real situations using a camera) Fig. 1 (a) or created by advanced physically based light renderings (used in lighting design phase), Fig. 1 (b). These images can then be processed using *Radiance*-based tools (*Findglare* (Ward-Larson and Shakespeare, 1998) or *evalglare* (Wienold and Christoffersen, 2006)) for deriving the relevant photometric quantities for the glare evaluation.

As convenient as this approach seems, it has complexities in attempts to define different components of the visual comfort metrics. One of these complexities is detecting the glare image pixels and deriving "glare sources", as they are perceived by human eye. Glare sources, their brightness and size are some of the main photometric quantities for the glare evaluation. The existing glare source detection algorithms consider any image pixel of luminance value that is larger than a threshold luminance as a "glare pixel". Different algorithms can determine this threshold luminance. As an example, the algorithm that is implemented in the existing tools uses the average luminance of a visual adaptation region and uses a multiplier x to derive the threshold luminance. The visual adaptation region is the fovea region of the eye for a presumed point of fixation in the space, e.g. the monitor screen. This algorithm is implemented in *evalglare* (default value= 5) and in *findglare* (default value =7).

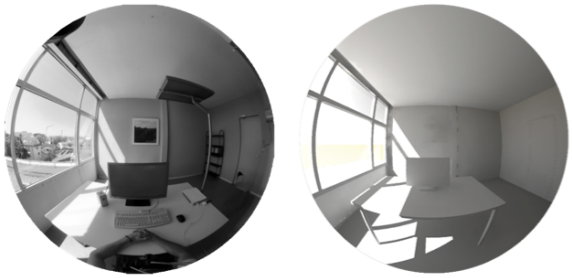

Figure 1 HDR luminance images: (a) captured by a CCD camera equipped with fisheye lens of a side-lit single office, (b) generated by physically based rendering of the same side-lit single office.

So far, there exists no study on accuracy or sensitivity of default values for the influential parameters in the existing algorithms. In this study we have made a sensitivity analysis on two important parameters: threshold multiplier x and the search radius r. In two series of experiments we took HDR images using a CCD camera under different lighting conditions and with different façade systems. We then analysed the images using 15 different combinations of the two parameters (threshold

multiplier *x* with 5 levels and search radius *r* with 3 levels of treatment) using the *evalglare* tool Fig. 2. The idea was to investigate if the different combinations of threshold multiplier and search radius make a significant difference on the resulting detected glare sources. Also by comparing the results to the gathered subjective assessments, we made an attempt to determine "right" detection parameter values.

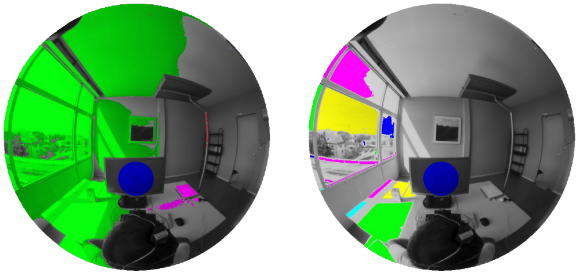

Figure 2 Using tools such as evalglare the captured images can be processed to derive relevant photometric quantities to glare metrics: (a,b) show two different parameter combinations. Random colours highlight the detected glare sources.

The preliminary results show that there is a significant effect of threshold on the lighting conditions and an effect of search radius on lighting conditions with shading systems. The results also show that the choice of the "right" detection parameters underlies some effects which cannot be explained so far. The consequence of this is that further investigations are needed and as long as no clear rule exists to choose the "right" detection parameters, the user of glare evaluation tools has to check the detected glare sources for each investigated situation.

BACKGROUND

Glare

The illumination conditions in the indoor environment can include situations that impair vision or create visual discomfort. One of these situations is known as glare which is usually marked by behaviours such as blinking, looking away, or shielding the eyes when encountering extreme contrast intensities, and if persistent results in visual fatigue. Glare was recognized as a visual phenomenon in the scientific literature for the first time in 1910 when it was characterised as "a more or less serious discomfort" (Parsons, 1910). This vague definition was later developed and categorized in a range from temporary visual reduction to extreme situations, e.g. retinal damage of the eye. Today, however, we have a better understanding of different types of glare sensation based on their spatial and temporal characteristics (Vos, 1999) and by their degree of seriousness (Stone, 2009). These different types can be categorised into two main temporal groups: rare and commonly experienced. Glare sensations such as flash blindness, paralysing glare, distracting glare and retinal damage glare fall into the first group, whereas conditions such as veiling glare (reflection), disability glare, and discomfort glare are more commonly experienced in indoor environments. Disability glare and veiling glare are caused by contrast reduction on either the retina or the surface of the object, e.g. computer screen or a glossy paper. Where disability and veiling glare are easier to recognise and quantify, discomfort glare, having been studied for more than 50 years, is less understood. The initial challenge with this phenomenon is that it only creates subjective negative responses with no immediate visual strain ((CIE), 1989) and no known physiological origins (Boyce, 2014).

Studies have associated discomfort glare with certain pupil fluctuation (Fry and King, 1975) and activities of facial muscles in the vicinity of the eye (Berman et al., 1994). However, it is not certain that these physiological observations are indications of a general discomfort, or whether they are created by the actual discomfort glare sensation (Stone, 2009; Howarth et al., 1993). So far, studies based on subjective assessments have been used to quantify discomfort glare by means of questionnaires. Most of these studies that have led to mathematical model for discomfort glare quantification were done under electrical lighting conditions, with the exception of one project under daylit conditions (Wienold and Christoffersen, 2006). Each of these glare models evaluate glare differently but they share a basic trend and draw upon the same four physical quantities: Luminance of the glare source (L_s), the solid angle of the glare source subtended at the eye (ω_s), the discomfort sensation the glare source induces based on its angular position in the FOV with respect to the gaze direction (P_i) and the adaptation luminance (L_a) EQUATION (1), (Boyce, 2014) .

$$Glare\ Perception = \frac{L_s^{exp_1}.\omega_s^{exp_2}}{L_a^{exp_3}.P_i^{exp_4}} \quad (1)$$

This form indicates that a brighter and larger source of glare in a high contrast room, which is closer to the gaze direction (within 10 degree but not at the gaze direction (Kim et al., 2009)), increases the risk of discomfort glare. Each component has a different exponent that varies for different discomfort glare equations.

The exponents 1-3, seen in EQUATION (1), are best-fitted empirical values. The inverse relation between luminance of the source and the luminance of the background indicates that higher background (or adaptation) luminance in the FOV can minimise discomforting effect of a prominent focused (small-sized) glare source. The Position Index (P_i) value is used in most of the common glare models with an

exponent 4 between 1 and 2. P_i s a complex equation which shows the change in discomfort based on the angular displacement of the glare source from a gaze line (Luckiesh abd Guth, 1949). It also highlights the sensitivity of different parts of the FOV to discomfort sensation (Iwata and Tokura, 1997; Kim et al., 2009). These four physical quantities can be derived from the HDR images through several image-processing algorithms.

HDR images & Glare Detection Parameters

HDR images are an accumulation of luminance values from a fixed point of view. These type of images allow for a larger difference between the brightest and the darkest areas of the registered image, thus representing a range of intensity levels that is similar to the real scene. This provides a basis for accurate, quick and inexpensive (Inanici, 2006) luminance-based light analysis. HDR images created by physically based lighting renderings are advance renderings of simulated 3D model of the architectural space. These renderings can be achieved by using tools such as *Radiance* (Ward-Larson and Shakespeare, 1998). On the other hand HDR photometry techniques (Rea and Jeffrey, 1990) with correct validations (Bellia et al., 2002; Inanici, 2006) and image processing methods (Wienold and Christoffersen, 2006) have proven to be a suitable method for evaluation of luminance distribution for the field of view (FOV) measurements as perceived in the real situation. Normally, a fisheye lens for a large FOV image capture is considered to cover the whole FOV of the human eye. Figure 1 (a) shows a 180° angular fisheye projection captured with a CCD camera with an HDR imaging setting. Three coordinates define each pixel in the camera coordination system and an RGB value is recorded. This type of images has been used in this study in all experiments to capture the light distribution during each experimental trial.

In the image-processing phase tools such as *evalglare* are used. *Evalglare*, which has been adopted in this study, is a tool to evaluate HDR images in order to derive the physical quantities relevant to more commonly used glare metrics such as Daylight Glare Index (DGI) and Daylight glare probability (DGP). The core algorithm of *evalglare* is dealing with the detection of the glare sources. The algorithm implemented in this tool goes through the image column by column in x and y direction, Fig. 3, and it checks every pixel luminance value and compares it with a luminance threshold (L_t).

L_t is determined by the product of the luminance of a reference area (a pre-defined zone, e.g. the monitor screen marked in Fig. 4 with a blue circle) and a threshold multiplier x. Another method to define L_t is the usage of a multiplier x on the average luminance of the entire image which is also implemented in this tool. The threshold multiplier x and the reference area are defined by the user. When the threshold luminance is determined, pixels of luminance value that are larger than L_t are detected as "glare pixels". Thereafter, the algorithm starts searching for similar pixels in the vicinity of the detected glare pixel. This search is done within a search radius r which is also pre-defined by the user. The detected pixels within the search radius are combined and defined as one glare source. The algorithm then continues to the next pixels. Ultimately, all the glare source patches within the image are detected.

For each detected glare source the luminance of the glare source L_S, the solid angle of the glare source ω_S

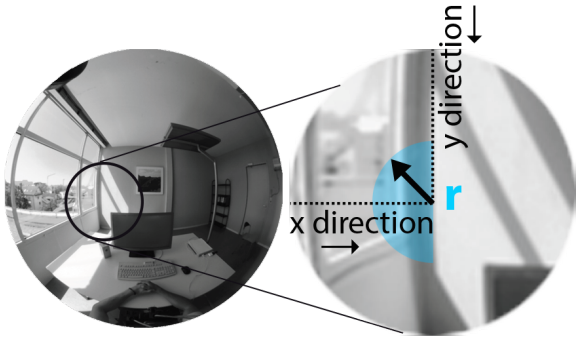

Figure 3 The algorithm searches the image pixels column by column in x and y direction.

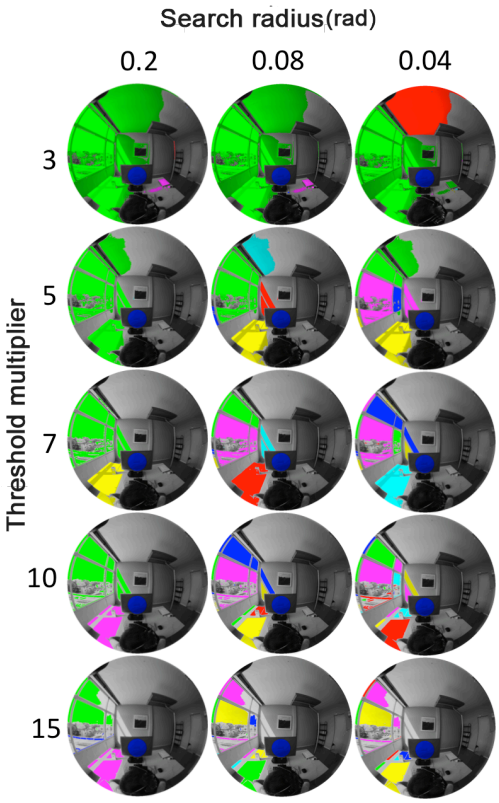

Figure 4 The 15 combinations are shown. Each image is an example of processed image for each detection combination. The coloured patches highlight the detected glare sources.

and the effect of angular position of each glare source to the optical axis of the image P_i are derived. The default values of the threshold multiplier x (default value =5) and the search radius r (default value =0.2 rad) are set intuitively based on the luminous environment of the underlying images of the *evalglare* development. Figure 4 shows the influence of the different settings of the two parameters x and r on the size and number of glare sources. The smaller x and the larger r is, the larger and fewer glare sources are detected. For a larger x and smaller r more glare sources of smaller size are detected.

METHODOLOGY

Two sets of experiments were performed. Both sets were done in the office like daylighting test facility at Fraunhofer ISE in Freiburg, Germany. A detailed description of the test facility can be found in (Wienold and Christoffersen, 2006). A range of lighting conditions were considered in order to create different glare situations. As the intention of this paper is not to investigate any specific glare metric but it is to show the effect of the glare detection parameters on the main variables of the glare metrics, we defined a new term "glare impact" for this purpose. This term was defined as a linear combination of L_S, ω_S divided by P_I for glare source i EQUATION (2).

$$Glare\ Impact = \sum_{i=1}^{n} \frac{L_{s,i} \cdot \omega_{s,i}}{P_i} \quad (2)$$

The glare impact served as the dependent variable. The independent variables were the two parameters threshold multiplier x and r and the lighting conditions. As a final step we compared the derived glare impact to the participants' ratings.

Experiments

The first experiments were executed in the years 2003-2005 and are described in detail in (Wienold and Christoffersen, 2006). The second experiments were performed July-October 2013. In both experiments participants were asked to perform a sequence of standardised office tasks while several measurements including photometric measurements and their subjective responses of the glare situation were acquired. The participants' subjective assessments were gathered based on a commonly used Likert scale for glare rating (Hopkinson, 1950). The main difference between the two sets of experiments is the achieved lighting conditions. Other important differences between the two experiments are:

1. Desk orientation: The first experiment had the desk oriented 45° towards the façade whereas the second one had it perpendicular to the façade.
2. Camera position: In the first experiment the camera was located exactly at the same position as the eye of the subject in the identical equipped "reference room" whereas in the second experiment the camera was located above the participant's head with displacement of 20 cm.

The two experiments created a large database of very different lighting situations.

Lighting condition

In the first experiments, nine lighting conditions were considered. The lighting conditions were achieved by varying two main settings. The first setting was the window size with 3 level of treatment: 25% (W1), 50% (W2), and 90% (W3) glazing fraction of the façade. The second setting was the shading systems also with 3 level of treatment: white venetian blinds convex slats (S1), high reflective specular blinds concave slats (S2) and a vertical blind with fully transparent foil slats (S3).

The shadings were pre-set in cut-off mode. The cut-off mode in case of venetian blinds was adjusted so

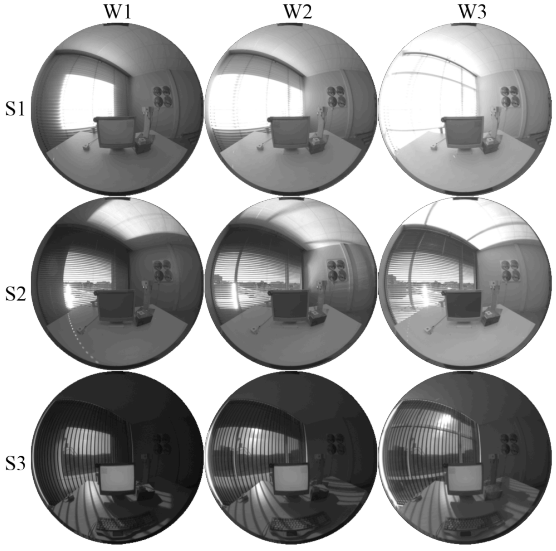

Figure 5 The 9 settings of experiment 1: The left column shows the 25% window size (W1), the middle column the 50% (W2) and the right column the 90% (W3). In the upper row the white venetian blinds (S1), the middle row the specular blinds (S2) and the third row the foil vertical blinds are shown (S3).

Table 1
Experiment 1: Lighting conditions.

EXPERIMENT 1: Each participant has evaluated one system with all three window sizes.	#
S1W1: White Venetian blinds, Small window (25%)	42
S1W2: White Venetian blinds, Medium window (50%)	43
S1W3: White Venetian blinds, Large window (90%)	43
S2W1: Specular Venetian blinds, Small window (25%)	41
S2W2: Specular Venetian blinds, Medium window (50%)	41
S2W3: Specular Venetian blinds, Large window (90%)	40
S3W1: Foil system, Small window (25%)	18
S3W2: Foil system, Medium window (50%)	18
S3W3: Foil system, Large window (90%)	18
Total number of images: 296	102

that the slats would just block the direct radiation while keeping the maximum view and in case of the foil slats, they were fully closed Fig. 5.
Table 1 shows the 9 lighting conditions with their specific shading system and number of acquired samples. Table 2 shows the mean values of different photometric quantities achieved by each condition. All tests were performed under clear sky conditions with the sun perpendicular to the façade.

Table 2
Experiment 1 Averaged photometric quantities

Conditions	$\bar{E}_v$ [lux]	$\bar{L}_a$ [cd/m^2]	$\bar{L}_s$ [cd/m^2]	$\bar{\omega}_s$ [sr]	$\bar{\#}Ls$
S1W1	2494	601	3309	0.58	7.4
S1W2	3514	943	4190	0.5	13.6
S1W3	4468	1265	5340	0.5	20.8
S2W1	3014	851	7603	0.5	17.4
S2W2	4122	1244	12088	0.5	23.2
S2W3	6093	194	22792	0.58	26.5
S3W1	347	78	5315	0.58	8.1
S3W2	330	83	3393	0.58	8.6
S3W3	513	135	5927	0.58	11.8

The second set of experiments addressed especially the occurrence of sun-patches in the room, without the use of shadings or change of window size. Six lighting conditions were achieved. Four of the lighting conditions were achieved under clear sky (LC1-4), one under overcast sky (LC5) and the last condition under electrical lighting condition with the window completely blocked and an electrical floor stand fixture is present in the scene (LC6) Fig. 6. The specification of each lighting condition and the number of participant are shown in table 3.
Table 4 shows the average photometric quantities for each lighting condition.

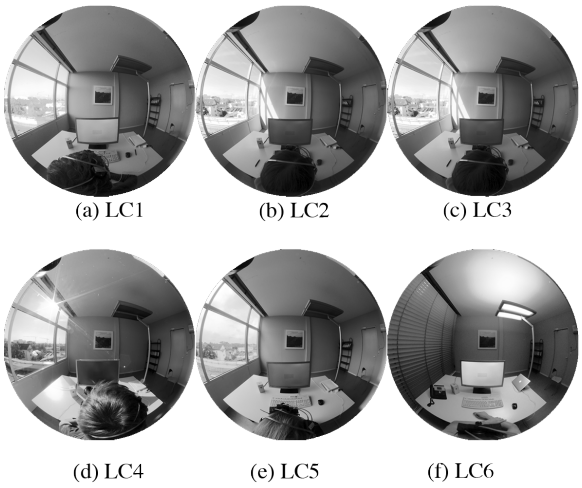

Figure 6 Six lighting conditions in experiments 2: (a) clear sky with no direct sunlight (LC1), (b) clear sky with direct sunlight on the opposite wall to the participant (LC2), (c) clear sky with direct sunlight on desk (LC3), (d) clear sky with sun in the scene (LC4), (e) overcast sky (LC5), (f) artificial light (LC6).

Table 3
Experiment 2: Lighting conditions

EXPERIMENT 2: Each participant has evaluated one system with	#
LC1: Clear sky, no system, no sun inside	23
LC2: Clear sky, no system, sun on the wall	16
LC3: Clear sky, no system, sun on the desk	11
LC4: Clear sky, no system, sun in the FOV,	15
LC5: Overcast sky, no system,	15
LC6: Artificial light, window covered	17
Total number of images: 97	97

Table 4
Experiment 2: Averaged photometric quantities

Conditions	$\bar{E}_v$ [lux]	$\bar{L}_a$ [cd/m^2]	$\bar{L}_s$ [cd/m^2]	$\bar{\omega}_s$ [sr]	$\bar{\#}Ls$
LC1	1200	300	4538	0.43	1.5
LC2	1800	600	2903	0.35	2.5
LC3	3000	1000	3919	0.33	4
LC4	5800	2500	45039	0.07	9
LC5	1000	400	2191	0.27	2
LC6	300	100	1064	0.08	1

RESULTS

Using each threshold multiplier *x* and search radius *r* combination, the captured images were processed in order to derive the luminance of the glare sources L_s, the solid angle of the glare source ω_s and the position Index P_i. To see the effect of the two parameters on the glare impact, we did an exploratory data analysis as the first step. Thereafter, in order to quantify the effects of the two parameters in the different lighting conditions, a three-way ANOVA was performed on glare impact as the dependent variable shown in equation 2.

Experiments 1

Figure 7 (a-c) show the mean value of glare impact for each threshold multiplier and lighting condition. The x-axis in each graph represents the threshold multiplier (3, 5, 7, 10 and15) and on the y axis the glare impact. In these graphs we can see that threshold multiplier 3, 7 and 15 in combination with smaller search radius gives lower glare impact values with a negative linear behaviour for the threshold multiplier. This means that a larger threshold multiplier with the smaller search radius gives a lower glare input values. Threshold 5 and 10 behave differently though. We can see that threshold multipliers 5 in combination with smaller search radius results in higher values.

Table 5
Three-way ANOVA results

Source	SS	df	MS	F	p
LC (a)	1.0×10^7	5	1.0×10^9	1361.9	0
Radius (b)	1.0×10^7	2	1.0×10^6	1.3	0.273
Multiplier(c)	5.8×10^8	4	2×10^8	259.5	0
a.b	1.3×10^7	10	1.2×10^6	1.58	0.105
a.c	1.3×10^7	20	3.8×10^7	48.37	0
b.c	1.3×10^7	8	3.2×10^6	0.99	0.4
Error	5.6×10^9	7000	7.9×10^5		
Total	1.2×10^10	7049			

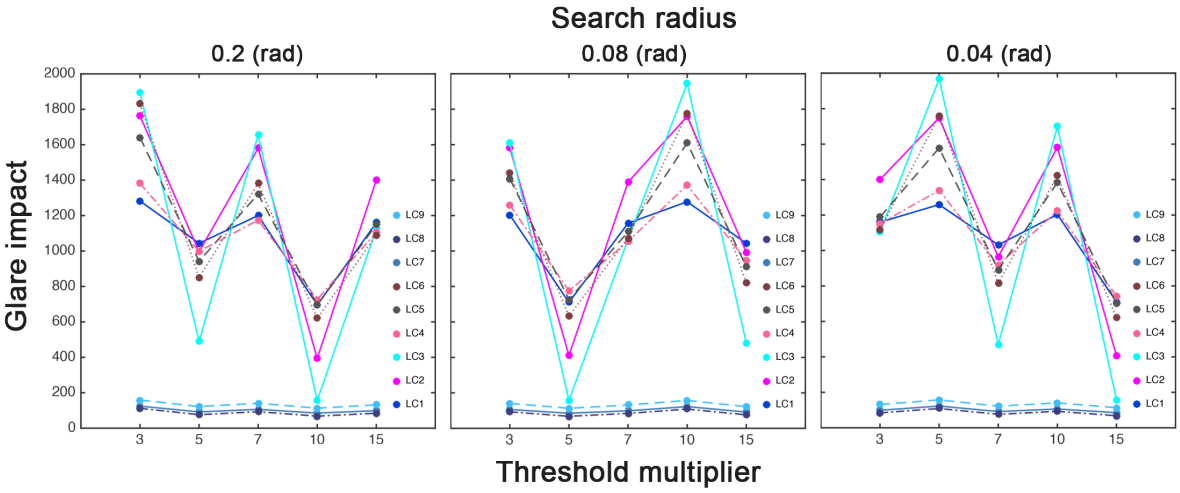

Figure 7: The mean value of glare impact (EQUATION 2) for each threshold multiplier is shown for: (a) radius 0.2 rad, (b) radius 0.04 rad, (c) radius 0.08 rad

On the other hand threshold 10 in combinations with mid range search radius 0.04 rad results in higher values than radius 0.2 rad or 0.08 rad. These results differ slightly for each lighting condition. Lighting condition S3W1, S3W2 and S3W3, have not been affected by the change of threshold multiplier or search radius.

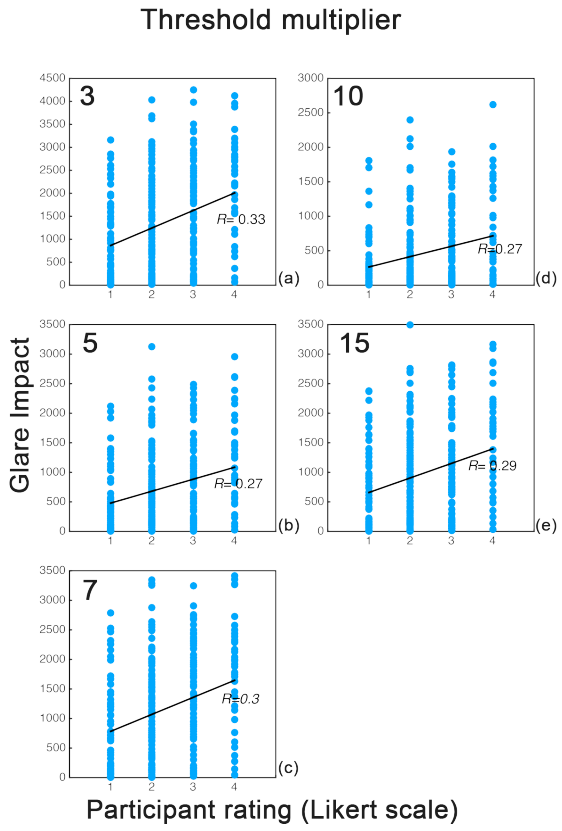

Figure 8: Pearson correlation for different threshold multipliers x and a radius r=0.2 rad. Data from all lighting conditions are used. All correlations are in a similar range.

The ANOVA results (F (4, 4489) = 259.5, $P <$ 0.0001) shown in table 5, demonstrates the highly significant effect of threshold multiplier. This effect is significant for all façade system used in this experiment ($F(4, 4489) = 48.37$, $P <$ 0.0001). There is also an interaction between search radius and threshold multiplier as discussed and seen in previous graphs and as seen in the ANOVA interaction results (F (4, 4489) = 0.99, $P <$ 0.0001). The correlation study with the participants' ratings were similar for all radiuses. Figure 8 shows these results for search radius 0.2 rad. The graphs are correlating the participant's ratings with the glare impact derived with each threshold multiplier. Threshold multipliers 3 with R value of 0.33 is more likely to derive glare impact values close to the participants' glare perception over the 9 lighting conditions.

Experiments 2

The mean value of glare impact as defined in equation 2 is shown in figure 9 (a-c). As in previous graphs the x-axis represent the threshold multiplier (3, 5, 7, 10 and15) and the y axis represents the glare impact. We can see that the different thresholds have an impact in the derived glare impact value. While all the thresholds are resulting in different glare impact values for different lighting conditions, threshold 7 results in much higher values. This trend is similar for the three radiuses for all lighting conditions.

Table 6
Three-way ANOVA results

Source	SS	df	MS	F	p
LC (a)	1.0×10^{7}	5	1.0×10^{9}	1361.98	0
Radius (b)	1.0×10^{7}	2	1.0×10^{6}	1.3	0.273
Multiplier(c)	5.8×10^{8}	4	2×10^{8}	259.5	0
a.b	1.3×10^{7}	10	1.2×10^{6}	1.58	0.105
a.c	1.3×10^{7}	20	3.8×10^{7}	48.37	0
b.c	1.3×10^{7}	8	3.2×10^{6}	0.99	0.4
Error	5.6×10^{9}	7000	7.9×10^{5}		
Total	1.2×10^{10}	7049			

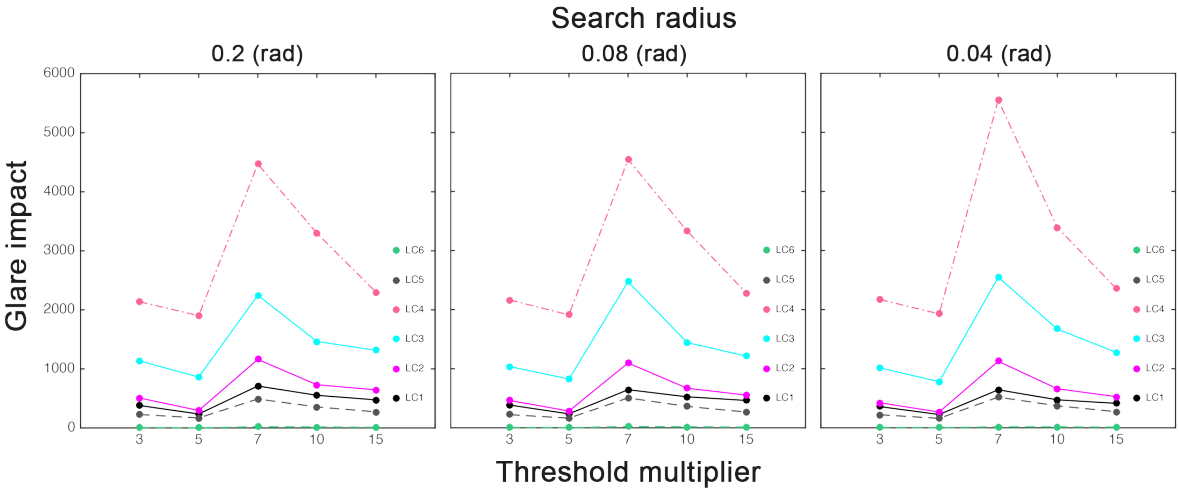

Figure 9: The mean value of glare impact for each threshold multiplier is shown for: (a) radius 0.2 rad, (b) radius 0.08 rad, (c) radius 0.04 rad.

When using radius 0.08 rad, Fig. 9 (c), together with threshold 7 we can see even higher glare impact values for lighting condition 4. Nevertheless, we can see in all three graphs that the search radius has less effect for these types of lighting conditions.

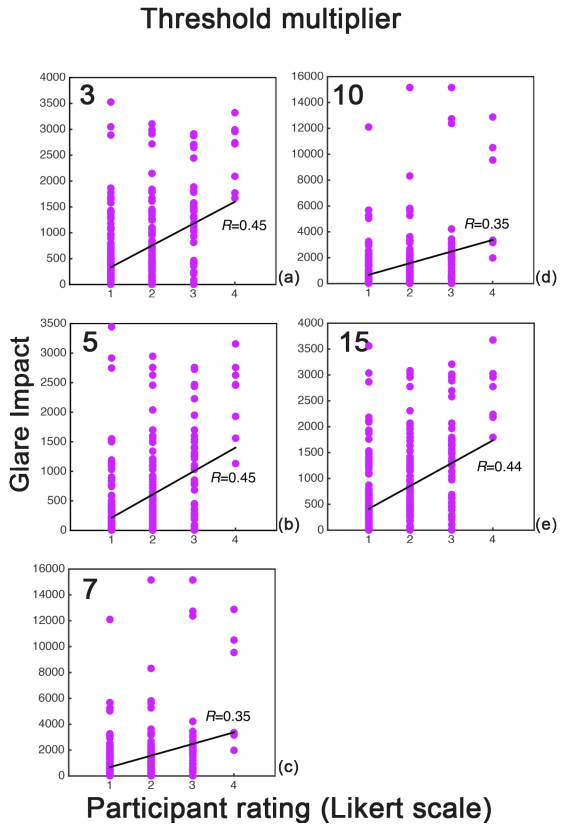

Figure 10: Pearson correlation for different threshold multipliers x and a radius r=0.08rad. Data from all lighting conditions are used. Threshold multiplier x =7 and x=10 show much lower correlation coefficient

The main difference here compare to the previous experiment is that no shading systems were used on the façade for creating the lighting conditions. For these cases the detection and combination of the glare pixels have not been affected.

ANOVA results ($F(4, 7000) = 259.5$, $P < 0.0001$) shown in table 6 confirms the significant effect of the threshold multiplier. Additionally, the significant interaction between the threshold multiplier and the lighting conditions are shown ($F(8, 20) = 0.48$, $P < 0.0001$). There is no effect of search radius or any interaction between search radius and lighting conditions or the threshold multiplier (All $P > 0.1$). Figure 10 compares the glare impact results with the participants' ratings for search radius 0.2 (as search radius has minimal effect on the detected glare impact values we are looking only at one search radius here). We can see that using threshold multiplier 7 and 10 glare sources with high luminance values are detected. But the correlation with user rating is lower. This can be due to the small size of this glare sources in these conditions or the have been out of the participants field of view, e.g. have been shaded by the window frame. But what is important is that the sensitivity of threshold 7 and 10 for detecting all glare pixels is much higher for this type of lighting conditions. Finally, based on the correlation study we can conclude that the threshold multipliers 3 and 5 ($R = 0.45$) are more likely to derive the subjectively accurate glare impact values.

CONCLUSION

Threshold multiplier x and search radius r are sensitive parameters for processing HDR images for deriving relevant photometric quantities to glare metrics.

Using *evalglare*, we processed 393 HDR images captured in two experiments that included 9 lighting conditions with different shading systems and 6 lighting conditions with different sun-patches. We

can see that for different light patterns in the room the sensitivity for the glare parameters vary. Also, some effects cannot be explained (e.g. the large difference between x=5 and x=7 for the second experiment). We assume, that this is related to some randomness within the patterns of the images. Importantly, we can see that the glare impact value which is shared by most commonly used glare metrics, is significantly affected by the choice of threshold multiplier. These effects are different for the 15 lighting conditions. Therefore, when setting these parameters for processing the images with different type of shading systems, the multiplier parameter has to be set carefully. From the investigated images the results suggest that threshold 3 result in glare impacts that correlates best with the user ratings for such lighting conditions. When using different shading devices, the selection of the search radius seems a more sensitive choice and can result in different glare impact outputs. But this sensitivity is not shown when comparing with the participants' ratings and there is need for further analysis to recommend an appropriate search radius when using shading systems. In future steps a study is recommended to validate these results in a controlled set up with focus on the goodness of different glare metrics. Additionally an approach is needed to get the glare evaluation more robust against the choice of detection parameters, so that an untrained user can perform glare evaluations without ending in

ACKNOWLEDGEMENT

The authors were supported by the École Polythechnique Fédéral de Lausanne (EPFL). The authors are grateful for the granted access to Fraunhofer ISE test facilities and thank the ISE staff and non-ISE participants

REFERENCES

Bellia, L., Cesarano, A., Minichiello, F., and Sibilio,S. 2002. Setting up a CCD photometer for lighting research and design. Building and Environment, 37(11):1099–1106.

Berman, S. M., Bullimore, M. A., Jacobs, R. J., Bailey, I. L., and Gandhi, N. 1994. An objective measure of discomfort glare, Journal of Illuminating Engineering Society.

Boyce, P. 2014. Human factors in lighting . Crc Press.

CIE, I. C. O. I. 1989. International Lighting Vocabulary. Central Bureau of the Commission Internationale de l'Eclairage, Kegelgasse , 27.

Clear, R. D. 2012. Discomfort glare: What do we actually know? Lighting Research and Technology.

da Silva, P. C., Leal, V., and Andersen, M. 2012. Influence of shading control patterns on the energy assessment of office spaces. Energy and Buildings, 50:35–48.

Dubois, M.-C. 2003. Shading devices and daylight quality: an evaluation based on simple performance indicators. Lighting Research and Technology, 35(1):61–76.

Fleischer, S., Krueger, H., and Schierz, C. 2001. Effect of brightness distribution and light colours on office staff. In The 9th European Lighting Conference. Proceeding Book of Lux Europa , pages 77–80.

Fry, G. A. and King, V. M. 1975. The pupillary response and discomfort glare. Journal of the Illuminating Engineering Society, 4(4):307–324.

Galasiu, A. D. and Veitch, J. A. 2006. Occupant preferences and satisfaction with the luminous environment and control systems in daylit offices: a literature review. Energy and Buildings , 38(7):728–742.

Hopkinson, R. 1950. The multiple criterion technique of subjective appraisal. Quarterly Journal of Experimental Psychology , 2(3):124–131.

Howarth, P., Heron, G., Greenhouse, D., Bailey, I., and Berman, S. 1993. Discomfort from glare: The role of pupillary hippus. Lighting Research and Technology, 25(1): 37–42.

Inanici, M. 2006. Evaluation of high dynamic range photography as a luminance data acquisition system, Lighting Research and Technology, 38(2): 123-136.

Iwata, T. and Tokura, M. 1997. Position index for a glare source located below the line of vision, Lighting Research and Technology , 29(3):172–178.

Kim, W., Han, H., and Kim, J. T. 2009. The position index of a glare source at the borderline between comfort and discomfort (BCD) in the whole visual field. Building and Environment, 44(5): 1017–1023.

Luckiesh, M. and Guth, S. K. 1949. Brightness in visual field at borderline between comfort and discomfort (BCD). Illuminating engineering.

Parsons, J. H. 1910. Glare, its causes and effects. The Lancet, 175(4508): 234–236.

Rea, M. S. and Jeffrey, I. 1990. A new luminance and image analysis system for lighting and vision equipment and calibration. Journal of the illuminating Engineering Society , 19(1):64–72.

Sivak, M., Flannagan, M., Ensing, M., and Simmons, C. J. 1989. Discomfort glare is task dependent. Technical report.

Stone, P. 2009. A model for the explanation of discomfort and pain in the eye caused by light. Lighting Research and Technology, 41(2):109–121.

Vos, J. 1999. Glare today in historical perspective: Towards a new CIE glare observer and a new glare nomenclature. Publications-Commission Internationale de l eclairage CIE , 133(1):38–42.

Ward-Larson, G. and Shakespeare, R. 1998. Rendering with radiance: the art and science of lighting visualization. Morgan Kaufmann Publishers Inc., San Francisco, CA, USA.

Wienold, J. and Christoffersen, J. 2006. Evaluation methods and development of a new glare prediction model for daylight environments with the use of CCD cameras. Energy and Buildings , 38(7):743-757.